Pergamon

0042-6989(95)00069-0

Vision Res. Vol. 35, No. 22, pp. 3103–3118, 1995

0042-6989/95 $9.50 + 0.00

Human Cones Appear to Adapt at Low Light Levels: Measurements on the Red–Green Detection Mechanism

A. CHAPARRO,* C. F. STROMEYER III,*† G. CHEN,* R. E. KRONAUER*

Received 8 July 1994; in revised form 23 December 1994; in final form 28 February 1995

Recent physiological evidence suggests that cones do not light adapt at low light levels. To assess whether adaptation is cone-selective at low light levels, the red–green detection mechanism was isolated. Thresholds were measured with a large test flash, which stimulated the L and M cones in different fixed amplitude ratios, on different colored adapting fields. Thresholds were plotted in L and M cone contrast coordinates. The red–green mechanism responded to an *equally-weighted* difference of L and M cone contrast on each colored field, demonstrating equivalent, Weberian adaptation of the L and M cone signals. The L and M cone signals independently adapted for illuminance levels as low as 60 effective trolands (e.g. M-cone trolands). Since this adaptation is entirely selective to cone type, it suggests that the cones themselves light-adapt. The red–green detection contour on reddish fields was displaced further out from the origin of the cone contrast coordinates, revealing an additional sensitivity loss at a subsequent, spectrally-opponent site. This second-site effect may arise from a net "red" or "green" signal that represents the degree to which the L and M cones are differently hyperpolarized by the steady, colored adapting field. Such differential hyperpolarization is compatible with equivalent, Weberian adaptation of the L and M cones.

Red–green detection Cone-selective adaptation Second-site adaptation

INTRODUCTION

The human daylight (cone) visual system maintains high sensitivity over an illumination range of more than one million-fold. Retinal processes re-equilibrate response sensitivity to each level of illumination, thus making the response to *contrast* largely independent of mean illumination (Shapley & Enroth-Cugell, 1984). Lamb (1985) has argued that independent adaptation of the three spectral classes of cones would make their contrast *contributions* independent of the spectral nature of the illuminant, thereby promoting color constancy (Ives, 1912; Normann, Perlman & Hallett, 1991)—an effect generally known as von Kries adaptation. It would be advantageous to have adaptation at the earliest stage (the cone photoreceptors) to prevent response saturation of either the cones or subsequent neural stages (Purpura, Tranchina, Kaplan & Shapley, 1990; Shapley, Kaplan & Purpura, 1993).

Surprisingly, however, recent recordings (Schnapf, Nunn, Meister & Baylor, 1990) of the photocurrent in single excised primate cones reveal only very slight adaptation (a 2-fold gain reduction) when exposed to high background illumination of ~2000 trolands. A recent study by Krauskopf and Gegenfurtner (1992) might seem to support this view that the cones do not light-adapt. They measured thresholds in humans for equiluminant red–green flashes (on the L–M axis) on colored fields of 400 td. Adapting field color ranged from green to orange, thus producing relatively large differential illumination levels for the L and M cones. Thresholds for equiluminant flashes changed little with adapting color, leading the authors to conclude that the L and M cones do not adapt under these conditions.

We used flashes that are not constrained to just the equiluminant axis, but rather flashes that could stimulate the L and M cones in any desired ratio (positive or negative). The red–green detection mechanism was isolated on colored fields that ranged between green and deep-red. We studied the red–green mechanism because it can be easily isolated—it has high sensitivity for stimuli like ours (King-Smith & Carden, 1976; Thornton & Pugh, 1983; Cole, Hine & McIlhagga, 1993; Chaparro, Stromeyer, Huang, Kronauer & Eskew, 1993), and it can be readily identified—for it responds to a simple linear difference of L and M test signals (Thornton & Pugh, 1983; Stromeyer, Cole & Kronauer, 1985; Calkins, Thornton & Pugh, 1992).

*Division of Applied Sciences, Harvard University, Cambridge, MA 02138, U.S.A.
†Department of Psychology, Harvard University, Cambridge, MA 02138, U.S.A.

By plotting thresholds in cone contrast coordinates, we could separate two adaptational processes which control sensitivity of the red–green mechanism. The first process appeared to be completely selective between the L and M cones, and was unaffected by a subsequent spectrally-opponent adaptational process. By correcting the actual threshold data for this latter "second-site" effect, cone-selective adaptation was revealed over the full illumination range. The two adaptation processes cannot be discerned with tests only restricted to the equiluminant axis.

The present method of isolating the red–green mechanism to study adaptation may have advantages over the earlier paradigms of Stiles (1978), which also clearly suggest there is cone-selective adaptation. By using the full gamut of test vectors within the cone contrast coordinates, we can better isolate the red–green detection mechanism. As we will show, a consideration of the slope and position of the red–green detection contour on different colored fields can reveal the two adaptational processes.

METHODS

Stimulus

A large (2.2° dia, 200 msec) test flash was presented in the center of a 6.2° uniform adapting field. The observer fixated between two continuously-presented, tiny black dots, presented ~0.5° above and below the center of the test disk. A large, long duration test flash was used to preferentially stimulate the red–green mechanism (Thornton & Pugh, 1983). The flash consisted of simultaneous increments and decrements of red and green lights (or vice versa), allowing us to stimulate the L and M cones in any desired amplitude ratio (positive or negative).

Apparatus

Stimuli were produced with an 8-channel Maxwellian view (Cole, Stromeyer & Kronauer, 1990). The stimulus consisted of red and green test disks (2.2°) and matched contiguous annuli, superposed on a brighter uniform adapting field (6.2°). The field appeared uniform (except for the fixation marks), since the edge between the test region and annulus was invisible. The adapting field was produced by light from a 50 W halogen lamp, passed through a monochromator. The red (671 nm) and green (550 nm) test disks and annuli were produced with light-emitting diodes (LEDs), filtered with interference filters. Test flashes were produced by modulating the test disks about their mean level, using 12-bit DACs, which were linearized with lookup tables.

The tests disks and annuli were formed with a mirror having a bare elliptical (test) area which appeared circular to the observer. The mirror was placed in a cuvette of index-matching silicone oil. A Maxwellian view lens imaged all lights on an artificial pupil and achromatizing lens (Bedford & Wyszecki, 1957), and a pair of relay lenses formed a 2.2 mm image of the artificial pupil in the observer's pupil. The observer was stabilized with a bite bar on a rigid *xyz* translator. Ocular chromatic aberration was corrected by adjusting the translator so that the red and green annuli appeared spatially coincident.

All light components were narrowband (8–10 nm full-bandwidth at half-height). Spectral calibrations of the lights were made in 1-nm steps with a radiometer and monochromator (2-nm BW) placed at the eyepiece of the optical system.

Threshold measurements

Thresholds were measured with a temporal two-alternative forced-choice procedure. After 2-min initial adaptation to the field, the observer initiated each trial with a button. Tones marked each temporal interval and gave feedback. Two to five Quest functions (Watson & Pelli, 1983), each of 30–60 trials, were randomly interleaved for each run. Each threshold estimate was determined by fitting results from 300 to 600 trials with the Weibull function

$$P(I) = 1 - \tfrac{1}{2}\exp[-(I/\alpha)^{\beta}],$$

where I, α and β represent respectively, stimulus intensity, threshold (82%-correct), and slope. For the detection measurements, only green or only red flashes were presented during each run.

Thresholds were also measured in several additional paradigms. In the *pedestal* paradigm, an identical suprathreshold luminance flash (the pedestal) was presented in both trial intervals; a spatially and temporally coincident, chromatic flash was added to the pedestal in one interval. The task was to select the interval with the chromatic test. The luminance pedestal matched the field chromaticity. In the *chromatic identification* paradigm, a single red or a single green chromatic flash was presented on each trial, and the observer attempted to choose the redder-appearing interval, i.e. the interval containing the red test when it was presented, and the blank interval when the green test was presented. In the analogous, *brightness identification* paradigm, either a brighter or darker chromatic flash was presented on each trial, and the observer attempted to choose the brighter-appearing interval. Our procedure overcomes response bias which would otherwise occur in measuring identification thresholds with an adaptive psychometric method (Chaparro, Stromeyer, Kronauer & Eskew, 1994).

Thresholds in absolute troland coordinates and the red–green detection mechanism

The measured spectral energy distributions of the lights were first multiplied by the Smith and Pokorny (1975) L and M cone fundamentals. Importantly, the relative heights of the L and M fundamentals have been set by Smith and Pokorny so that their sum is equivalent to the luminosity function,

$$\text{Judd-corrected } V_\lambda = L_\lambda + M_\lambda.$$

Thus the illuminance of a light, specified in trolands, can be apportioned between the L and M cones (Boynton, 1986).

We first represent the threshold measurements in L and M troland coordinates. One L td and one M td produce about 18 and 11 quantal catches per sec in a foveal L and M cone, respectively. (This is based on assumptions of 0.6 ocular transmission, 0.4 peak photo-pigment density, 16,800 cones/deg^2 for the foveaola, and that the relative peak sensitivities of the Smith and Pokorny L and M cone functions reflect the relative number of L vs M cones.) The test flash produces an illuminance change of Δ trolands, apportioned between the L and M cones, ΔL td and ΔM td (Boynton, 1986). Test flashes plotted along the horizontal axis (Fig. la) produce increments and decrements in the L cones alone (with the M cones "silenced"); similarly, flashes plotted along the vertical axis produce changes in the M cones alone.

Flashes on the equiluminant axis (135–315° axis) produce no illuminance change by definition (of the V_λ function), since the troland changes owing to the L and M cones exactly cancel each other. This physical equiluminant axis does not necessarily correspond to the psychophysically-determined equiluminance axis on each adapting field. The axis for psychophysical equiluminance must be *parallel* to the luminance detection contour on each colored adapting field, and the slope of contour varies with the color and intensity of the adapting field (Eisner & MacLeod, 1981). We first consider this physical (V_λ) equiluminant axis, so as to compare our results with those of Krauskopf and Gegenfurtner (1992).

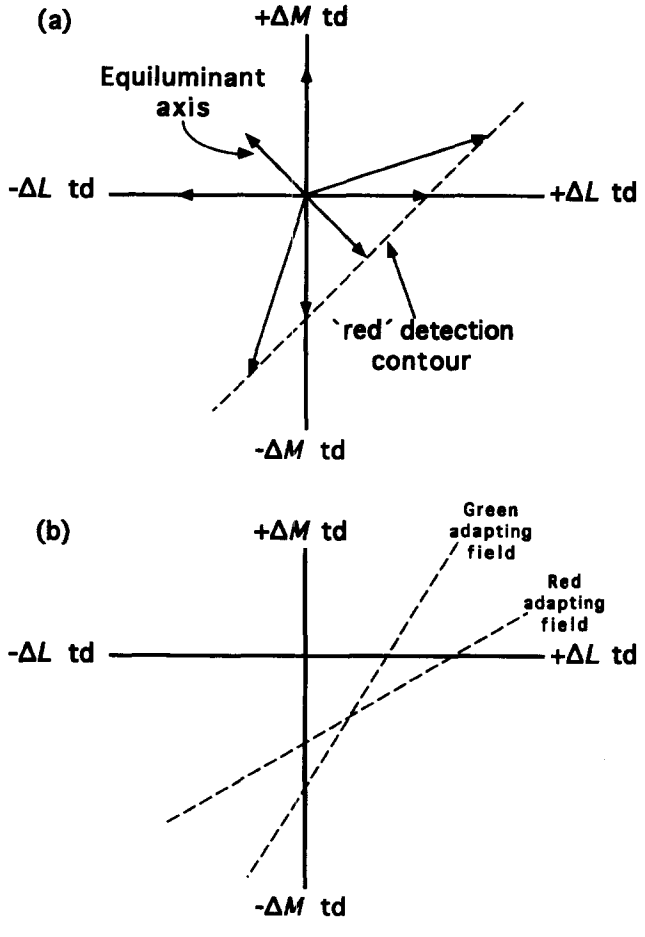

FIGURE 1. (a) L and M troland coordinates for test flash. The test flash (a vector) produces an illuminance change, in trolands, apportioned between the L and M cones. Vectors on horizontal axis stimulate L cones alone, while vectors on vertical axis stimulate M cones alone. On the equiluminant (135–315°) axis, the flash produces *no* illuminance change since the L and M troland changes are of equivalent magnitude but opposite sign. The vectors at 135° and at 315° represent, respectively, green and a red equiluminant flash. Hypothetical "red" detection contour is drawn through vectors for threshold red flashes detected by red–green mechanism. (b) On the red adapting field, the red detection contour is expected to have a flatter slope, since the L cones may adapt more than M cones—elevating thresholds along the L-cone axis. On the green field the contour is expected to be steeper, since the M cones may adapt more.

The dashed contour in Fig. la represents the hypothetical "red" detection contour for the red–green mechanism, measured with a wide range of test flashes. Each vector depicts the ΔL and ΔM td components of a threshold-level flash, with the adapting field represented at the origin. The red–green mechanism responds to a linear difference of L and M test stimuli. The red contour is represented by the equation,

$$a\Delta L \text{ td} - b\Delta M \text{ td} = \text{constant},$$

with positive coefficients a and b. All flashes along the contour produce a response of red polarity. A contour for green polarity would be represented by a similarly positioned parallel contour, on the opposite side of the origin.

Figure lb shows how the slope of the red contour may change on a red adapting field and on a green field. The red field may adapt the L cones more than the M cones, thus elevating thresholds along the L-cone axis. In contrast, the green field may steepen the contour by elevating thresholds along the M-cone axis. Our results indicate that on each field, the slopes of the red detection contour and the green contour are similar, and approximately symmetrically positioned relative to the origin.

RESULTS

Red–green detection contours on various adapting fields

Figure 2 shows both green and red detection contours measured on 400 td adapting fields (top panels) and 3000 td fields (bottom panels). The specified field wavelength is for the entire field (main adapting background plus LEDs, calculated from the Smith and Pokorny fundamentals). Test flashes on the upper contour in each panel (2nd quadrant) generally appeared greenish at threshold, and flashes on the lower contour (4th quadrant) appeared reddish. Straight contours are drawn through flashes assumed to be detected by the red–green mechanism. The fitted red and green contours for each field condition were constrained to have the same slope, but with the intercepts free to vary. The symmetric positions of the red and green contours from the origin indicate equal sensitivity to red and green chromatic flashes (Stromeyer *et al.*, 1985; Cole *et al.*, 1993).

The flashes were assumed to be detected by the spectrally-opponent, red–green mechanism for three reasons. First, the thresholds are well fit by straight

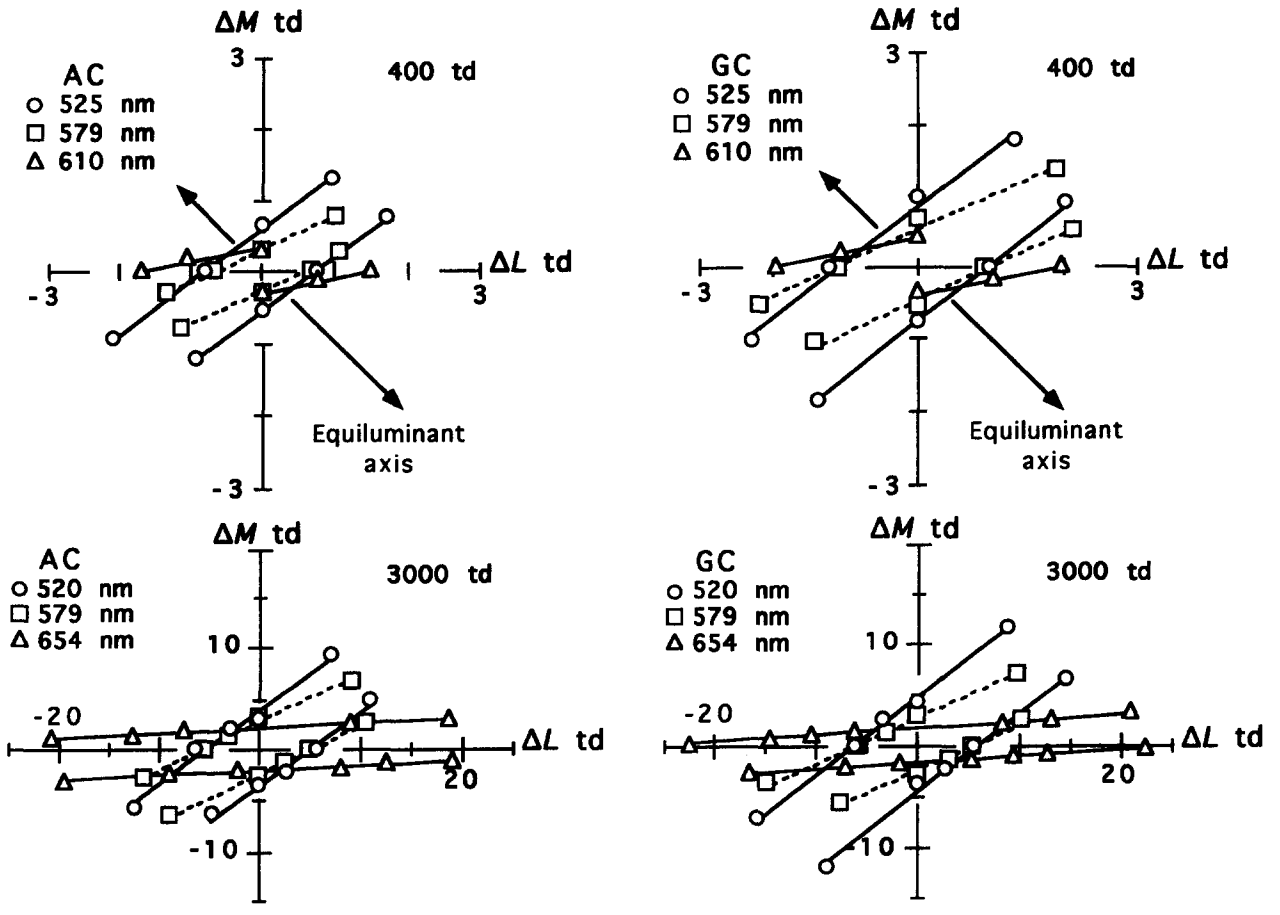

FIGURE 2. Detection contours for red–green mechanism measured on 400 td (top panels) and 3000 td fields (bottom panels). Within each panel, the upper contours represent green response polarity and the lower contours represent red polarity. Straight lines of the *same* slope are fit for both polarities, with the intercepts free to vary.

contours of positive slope, indicating detection by a mechanism with opponent L and M inputs. Second, the flashes generally appeared red or green at threshold, consistent with previous studies showing the flashes can be chromatically discriminated with the same accuracy that they are detected (Cole *et al.*, 1990). (We present such data in control experiments.) Third, other studies have shown that the detection contour slope predicts suprathreshold red–green hue equilibria (Thornton & Pugh, 1983) and suprathreshold indiscriminability contours (Calkins *et al.*, 1992).

Selective cone adaptation is shown by the fact that the contours are steepest on a green field and most flat on a red field—as predicted (Fig. 1b). From the contours in Fig. 2, we determined the thresholds along the L-cone axis, the M-cone axis and the equiluminant (135–315°) axis. These thresholds are shown in Fig. 3, for both the dim and bright fields. Krauskopf and Gegenfurtner (1992) observed that the equiluminant thresholds changed little with field color, thus concluding there is little cone adaptation in the red–green mechanism. We also observe rather little variation in the equiluminant thresholds. However, the thresholds for the pure L-cone and pure M-cone flashes change considerably more with field color. As shown in Fig. 2, the contours tend to rotate around an approximately *common* point on the equiluminant axis—thus restricting measurements to the equiluminant axis is the least sensitive place to discern the effects of adaptation (Eskew, Stromeyer & Kronauer, 1992).

The results as displayed in Fig. 3 are somewhat unexpected. The L-cone thresholds change markedly with field wavelength, whereas the M-cone thresholds change little. This is paradoxical since varying the adapting field from 525 to 654 nm decreases the mean M-cone stimulation by 8-fold and increases the mean L-cone stimulation by only 2-fold. It will be shown that when we correct the data for the second-site effect, this puzzling aspect of the data disappears and the data conform to the prediction of cone-selective adaptation.

We next transformed our results from the L and M troland (absolute) coordinates to coordinates of L and M cone *contrast*. This will reveal whether the L and M cones signals adapt independently on each colored field, so that their contrast contributions are equal within the red–green mechanism. The data points from Fig. 2 are replotted in Fig. 4, using cone contrast coordinates, $\Delta L/L$, $\Delta M/M$. For this transformation, the incremental test components, ΔL td and ΔM td are, respectively, normalized by the mean field stimulation for that cone type (L td or M td), and plotted along the x and y axes, respectively, in Fig. 4. This new transformation reveals

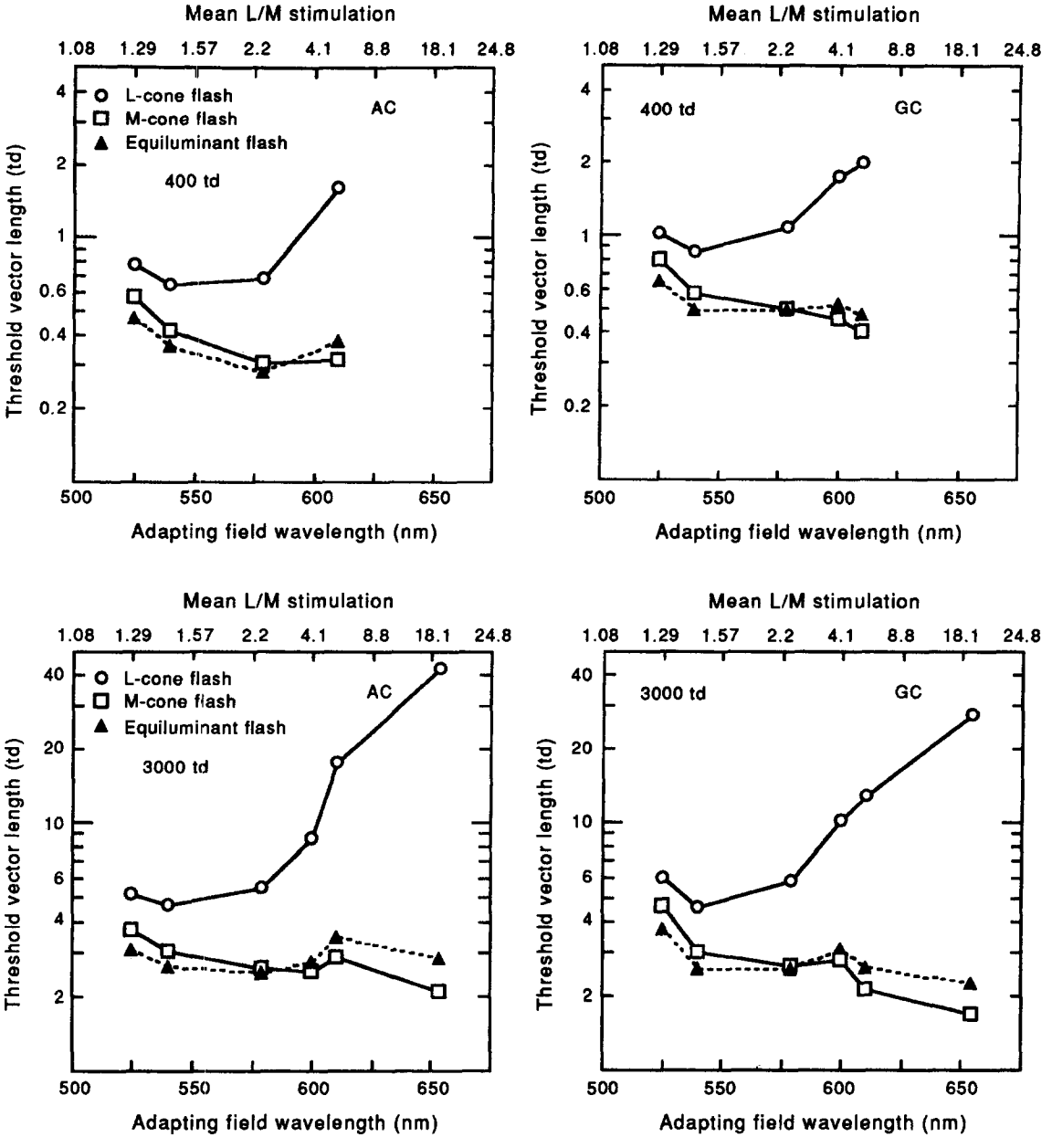

FIGURE 3. Replotted features of the data from Fig. 2 (top panels—400 td fields; bottom panels —3000 td fields): thresholds along the L-cone axis, along the M-cone axis and along the equiluminant axis (assessed from fitted contours, Fig. 2). Results for additional fields are also depicted.

two adaptational processes. First, the detection contours in cone contrast coordinates all have slopes of ~ 1.0, indicating that the red–green detection mechanism responds to a linear difference of equally-weighted cone contrast, $a\Delta L/L - b\Delta M/M = \text{constant}$ $(a = b)$. This shows that the L and M signals individually adapt and conform to Weber's law. (For sufficiently weak fields, a short-fall from Weber's law is likely and the contours would deviate from a slope of 1.0, even if the adaptation was completely cone-selective.) With no cone-selective adaptation, the slope in Fig. 4 would have varied over a 6-fold range on the dim fields, since there was a 6-fold variation in the M/L background stimulation. The L and M cone contrast contributions are equal even on the bright, deep-red (654 nm) field which produces a 19 to 1 difference in mean L and M cone stimulation.

The results in Fig. 4 also provide evidence for a second-site effect—the detection contours on reddish fields are shifted outward, while maintaining a slope of ~ 1.0. This reflects an additional decrease of chromatic sensitivity (over and above the cone-selective adaptation) dependent on field color. The red field, by producing a large L/M field ratio, could partially saturate the response of the red–green detection mechanism at an opponent site (Pugh & Mollon, 1979; Wandell & Pugh, 1980; Stromeyer *et al.*, 1985). Alternatively, the red field may reduce the response gain in retinal P cells (Shapley & Kaplan, 1990). Figure 5 shows this second-site effect as a function of field color, for both the dim

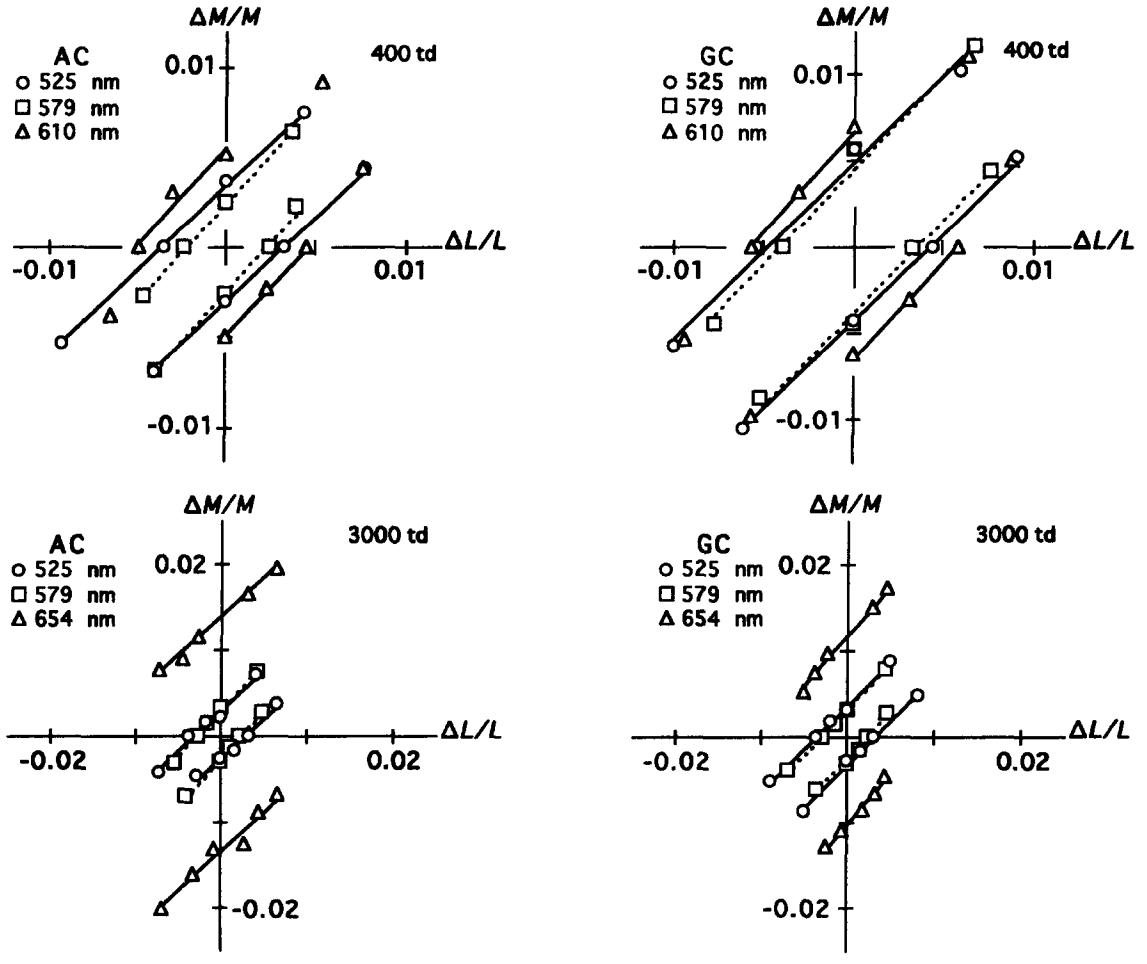

FIGURE 4. Chromatic thresholds from Fig. 2 converted to cone contrast coordinates. For each threshold point in Fig. 2, the ΔL td value was divided by the L td field stimulation and the ΔM td value was divided by M td. In the present figure, straight contours are fitted to thresholds assumed to be detected by the red–green mechanism—again the slopes for red and green flashes were constrained to be the same, with the intercepts free to vary. Two adaptational processes are revealed: the contours have slope ~ 1.0 indicating that L and M *contrast* contributes equally to detection on each colored field (cone-selective adaptation), and the contours are further displaced from the origin on reddish fields (second-site adaptation).

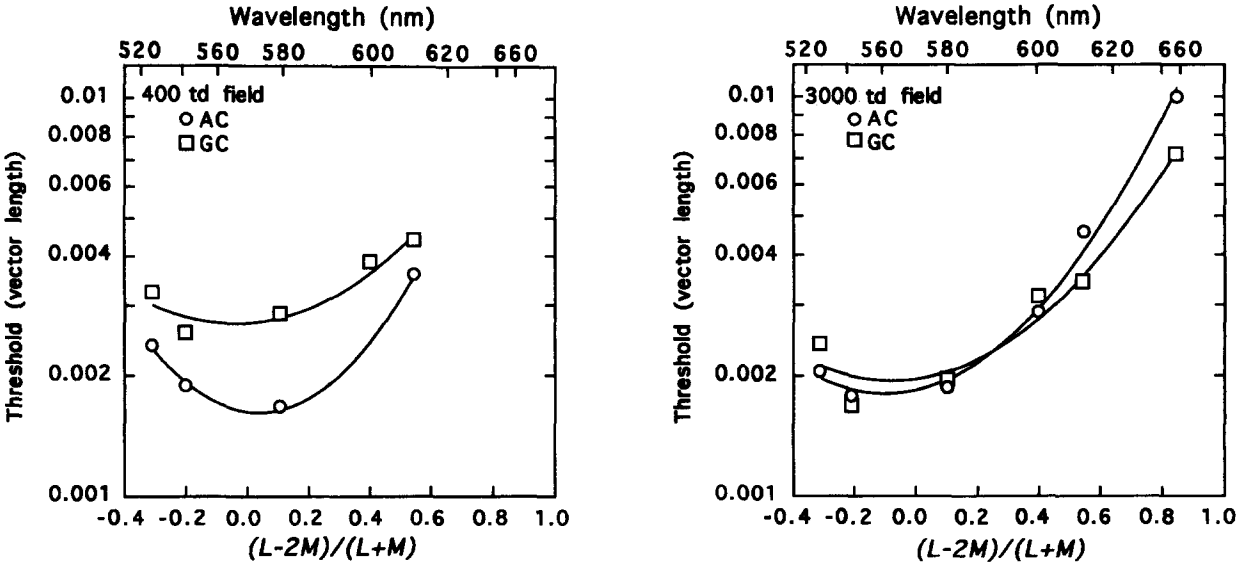

FIGURE 5. The second-site effect for the 400 td fields (left panel) and 3000 td fields (right panel). Thresholds represent the mean vector length (along the 135–315° axis) to the red contour and to the green contours in Fig. 4. Bottom axis specifies field color in units of Nagy *et al.* (1987)—zero corresponds to a "neutral" greenish-yellow field of ~ 570 nm.

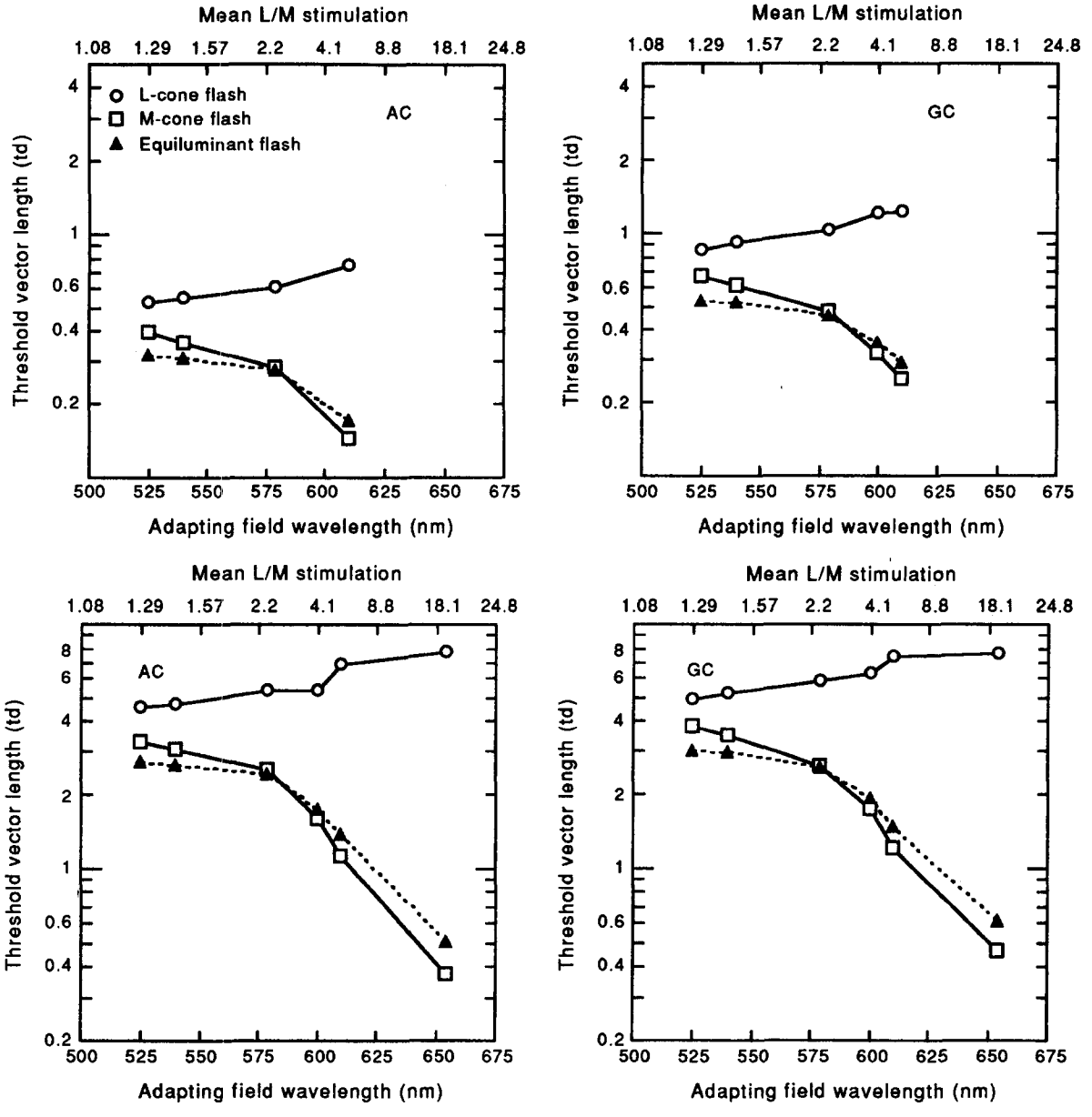

FIGURE 6. Data of Fig. 3 (thresholds in the original troland coordinates) now corrected for the second-site effect—400 td fields (top panels); 3000 td fields (bottom panels). These data thus reveal the cone-selective adaptation, occurring *before* the second-site effect. The original detection contours (Fig. 2) were scaled by the reciprocal of the second-site effect in Fig. 5 (normalized to 1.0 for the ~570 nm field condition). (The vertical axis in troland units is thus correct for only the ~570-nm field condition) for all other fields the vertical axis specifies the threshold in trolands assuming there is *no second-site effect*—since it is now compensated for.)

and the bright fields. The ordinate depicts the mean vector length to the red and to the green contours along the 135–315° axis (Fig. 4) in the cone contrast coordinates. The abscissa depicts the field color in units used by Nagy, Eskew and Boynton (1987). The curves are best-fitting, second order polynomials. Thresholds are lowest on yellow fields, and they rise slightly on green fields and strongly on red fields. These results are consistent with earlier findings showing that the "second-site" is least polarized on a yellow field (Boynton & Kambe, 1980; Wandell & Pugh, 1980; Nagy *et al.*, 1987; Stromeyer *et al.*, 1985; Romero, García, Jiménez del Barco & Hita, 1993). In contrast to these chromatic thresholds, our luminance thresholds on the 45–225° axis of the cone contrast coordinates (not plotted) varied little and unsystematically with field color, with a SD of ~16% for both observers (cf. Stromeyer *et al.*, 1985). The fact that field color has so little effect on the luminance thresholds but a large effect on the chromatic thresholds, provides evidence that the flashes are detected by different mechanisms.

The second-site effect accounts for the paradoxical results in Fig. 3—recall that the L-cone thresholds were strongly affected by field color but the M-cone thresholds were little affected—just the opposite of what we might expect based solely on cone-selective

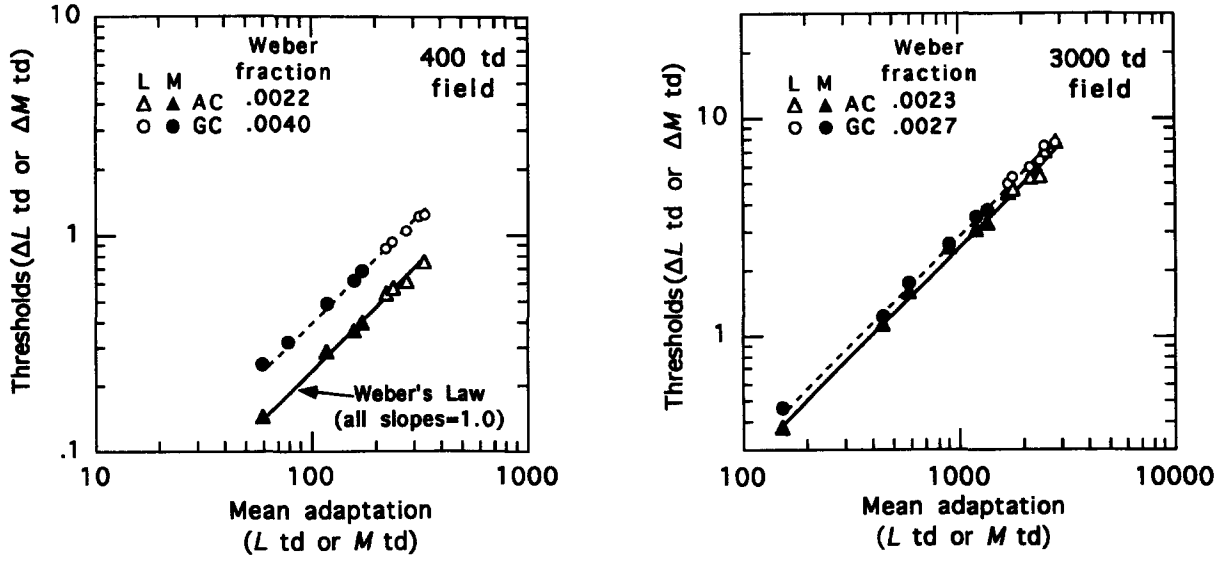

FIGURE 7. The range of light intensities over which Weber's Law adaptation occurred for the L and M cones. The vertical axis plots the incremental threshold, ΔL td or ΔM td (corrected for the second-site effect, Fig. 6), and the horizontal axis plots the mean field stimulation associated with that incremental threshold—mean L stimulation for ΔL, and mean M stimulation for ΔM. For observer G. C., overall sensitivity was slightly lower on the dimmer fields, yielding a slightly higher Weber fraction.

adaptation. Second-site adaptation causes both the L-cone and the M-cone thresholds to rise strongly on the red adapting fields. Figure 6 shows these earlier results (from Fig. 3) now corrected for second-site adaptation, thus revealing the adaptation *before* the second-site. This correction was made by recomputing the position of the red–green contours in Fig. 2, multiplying the coordinates of the contours by the reciprocal of the second-site effect in Fig. 5 (normalized to a value of 1.0 for the ~570 nm field condition). Figure 6 reveals a shallow rise of the L-cone thresholds on red fields, and a correspondingly steep decline of the M-cone thresholds, as expected on the basis of cone-selective adaptation.

Having corrected the L-cone and M-cone thresholds for the second-site effect (Fig. 6), we can now examine over what light intensity range the thresholds obey Weber's Law. Figure 7 shows that the incremental thresholds for each cone class, ΔL td (open symbols) and ΔM td (filled symbols), rise equivalently, in proportion to the mean field stimulation for that class of cones. Note that the different colored fields produce a greater range of mean stimulation for the M cones than the L cones, because M cone sensitivity changes more radically than L cone sensitivity with field color. Weberian, cone-selective adaptation is clearly present over the full range of adapting illumination, down to 60 M td. This Weberian behavior is not an artifact of the second-site correction, since the correction only affects the position of the red–green contours and *not* their slopes. It is the slope that reflects the relative sensitivity of L and M on each colored field. The slope remains ~1.0 with or without the second-site correction.

Control experiments—separating the luminance and red–green mechanisms on the deep-red adapting field

The second-site effect is strongest on the bright red (3000 td, 654 nm) field, reducing the sensitivity of the red–green mechanism relative to the luminance mechanism, and thus making it difficult to discern the red–green mechanism. We conducted two sets of supplementary experiments on the bright red field to provide proof of independent luminance and chromatic mechanisms. The first set of experiments provides evidence that the chromatic mechanism signals color alone. The second set establishes that the sensitivity of the luminance mechanism can be manipulated largely independently of the chromatic mechanism.

Test for chromatic and brightness identification by the red–green detection mechanism. If the red–green contour represents the action of only the chromatic mechanism (with two response polarities), then red vs green flashes should be identified as well as they are detected. The circles in Fig. 8 represent the original detection thresholds on the red field, whereas the triangles

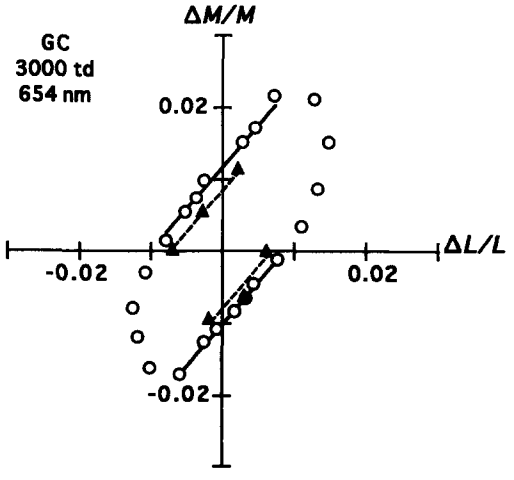

FIGURE 8. Chromatic identification thresholds for red vs green flashes (triangles) measured on the 3000 td, 654 nm red adapting field. Circles depict the original detection thresholds.

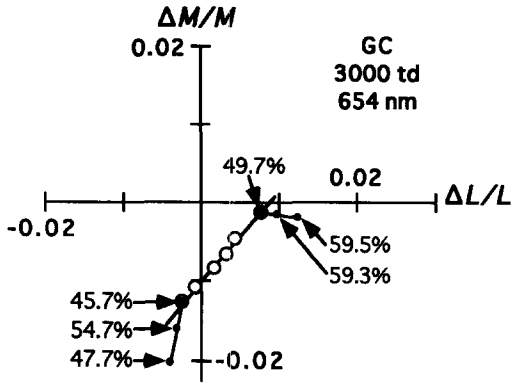

FIGURE 9. Poor brightness discrimination for flashes detected by red mechanism. Open circles depict the original red detection contour. Flashes represented by the two filled circles lying on this contour are poorly discriminated in brightness (near chance). The other filled circles show similarly poor discrimination for pairs of flashes either 0.1 log units above detection threshold or 0.2 log units above threshold.

represent chromatic identification thresholds (Methods) representing the discriminability of red flashes (fourth quadrant) vs green (second quadrant). The identification thresholds are actually slightly lower—they were collected later when the observer was more practiced. The identification thresholds have a slope like the original detection contour.

The open circles in Fig. 9 show the original detection thresholds of the red flashes. Filled circles show brightness discrimination performance, where the observer was asked to identify the brighter of the two red flashes, presented as test vectors of 351° vs 259° in cone contrast coordinates—either at detection threshold, or 0.1 log unit above the threshold or 0.2 log unit above threshold. Performance was near chance, suggesting that the flashes looked equally red but indistinguishable in brightness. Calkins *et al.* (1992) observed that various red flashes detected by the red–green mechanism could be raised as much as 0.7 log units above detection threshold before the luminance mechanism intervened and made the flashes distinguishable—in their study there was better isolation of the red–green mechanism (they used a low-frequency flash on a yellow adapting field).

Using a luminance pedestal to suppress the luminance mechanism independently of the red–green mechanism. The objective is to reveal the red–green mechanism over a broader vector range by using a suprathreshold luminance pedestal which masks the luminance mechanism while weakly facilitating the red–green mechanism (Cole *et al.*, 1990). The open circles in Fig. 10 show the original detection thresholds, while the filled circles show the red contour remeasured on a luminance pedestal of 6× threshold. For both observers the slope of the latter contour is ~1.0. For observer G.C. the measurements show chromatic detection to extend well into the first quadrant (since the pedestal *masks* the luminance mechanism).

Luminance mechanism measured on the red field. Figure 11 provides evidence that we can independently

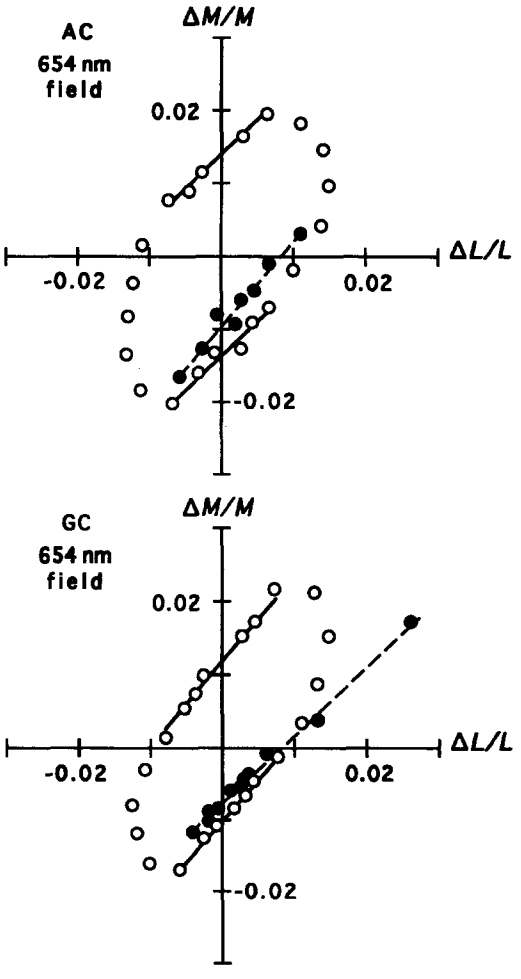

FIGURE 10. Open circles show the original detection contours on the red field, and filled circles show thresholds in the presence of a luminance pedestal of 6× threshold—which slightly facilitates red detection and masks luminance detection.

manipulate the luminance mechanism, thus further indicating there are separate red–green and luminance mechanisms. The open circles show the original detection thresholds for the 200 msec flashes. Diamonds depict the luminance contour measured with short (40 msec) flashes. This shorter duration causes the luminance threshold (on the 45° axis) to rise only 0.4×. The red–green thresholds would be expected to rise about 3×, owing to the longer temporal integration of the chromatic mechanism (Chaparro *et al.*, 1993; Stromeyer *et al.*, 1985), but there was insufficient test light to measure chromatic thresholds at this brief duration. The triangles depict the luminance contour measured with the 200 msec flashes, presented on a luminance pedestal of 0.7× threshold, which facilitates the luminance mechanism via subthreshold summation.

The two dashed luminance contours have a slope of about −3, indicating that on the red field the L cones contribute more strongly to the luminance mechanism than do the M cones. This is surprising in light of Eisner and MacLeod's (1981) observation that bright red adapting fields suppress the L cone input to the

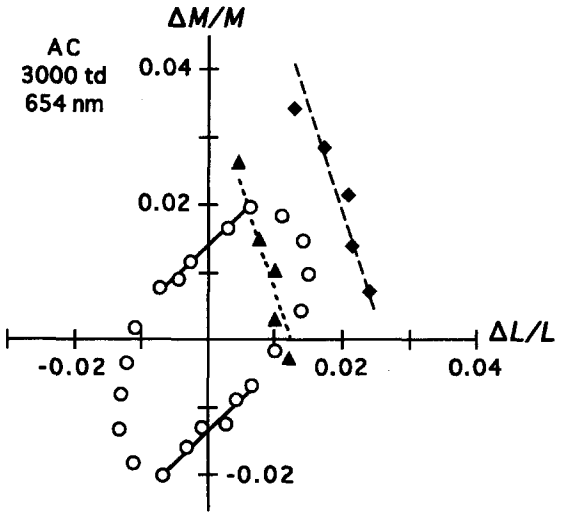

FIGURE 11. Open circles show the original detection thresholds on the red field. Diamonds depict the luminance detection contour for a brief (40 msec) test flash. Triangles depict the luminance contour for the original (200 msec) flashes on a luminance pedestal of 0.7 × threshold, which produces subthreshold summation in the luminance mechanism.

luminance mechanism. However, they used 15 Hz flicker, and Swanson, Pokorny and Smith (1988) remark briefly that the L-cone suppression is reduced at lower temporal frequencies, supporting the present observations.

DISCUSSION

Isolation of the red–green detection mechanism

We believe the approximately straight sections of our detection contours, where detection is controlled by an equally-weighted difference of L and M cone contrast on *each* colored field, represent the action of the red–green mechanism. Other measurements made on a yellow field strongly support this view. Spatial and temporal summation is very different as measured on the −45° chromatic axis vs +45° luminance axis (Chaparro *et al.*, 1993). Red and green chromatic flashes can be discriminated as well as they can be detected (Cole *et al.*, 1990; Chaparro *et al.*, 1994). Suprathreshold flashes lying on a line parallel to either the red *or* green contours presumably stimulate only the red–green mechanism for the flashes are *indiscriminable* from each other until of sufficient intensity to stimulate a second, luminance mechanism (Calkins *et al.*, 1992). On a yellow field, Calkins *et al.* found a range of red vectors and a range of green vectors which were perfectly discriminable from each other (as well as from an incremental luminance vector—on the +45° luminance axis), and they showed that the green flashes were indistinguishable, as were the red. The latter flashes were all at a constant multiple of detection threshold. This strongly supports the view that separate mechanisms mediate detection of these different categories of flashes. The present study shows that on a red field the chromatic mechanism is less sensitive than on a yellow field, but control experiments indicate that we have isolated the chromatic mechanism on the red field, since the results for chromatic and brightness discrimination are similar to those of Calkins *et al.* obtained on a yellow field. A further clear distinction between the red–green mechanism and the luminance mechanism is seen in the effect of the chromatic field on threshold sensitivity: changing the field color leaves the luminance threshold on the +45° axis largely unchanged, but the chromatic threshold is strongly elevated by reddish fields (cf. Stromeyer *et al.*, 1985, 1987).

Related studies

Krauskopf and Gegenfurtner (1992) observed that equiluminant red–green thresholds were approximately constant on 400 td adapting fields of 550–605 nm. Figure 12 plots their equiluminant thresholds, as well as ours for both the dim and bright fields. The thresholds are normalized to 1.0 for yellow adaptation—the abscissa represents the adapting field color as in the MacLeod–Boynton (1979) chromaticity diagram. Over the field range where the two studies overlap, there is relatively little variation in threshold.

This contrasts with the many studies showing that *equiluminant* red–green thresholds rise significantly as the field deviates away from yellow in either the green or red direction (MacAdam, 1942; Brown & MacAdam, 1949; LeGrand, 1949; Wyszecki & Fielder, 1971; Boynton & Kambe, 1980; Nagy *et al.*, 1987; Romero *et al.*, 1993). These studies typically employed a *small* (2°) bipartite field. The observer either adjusted a knob so the

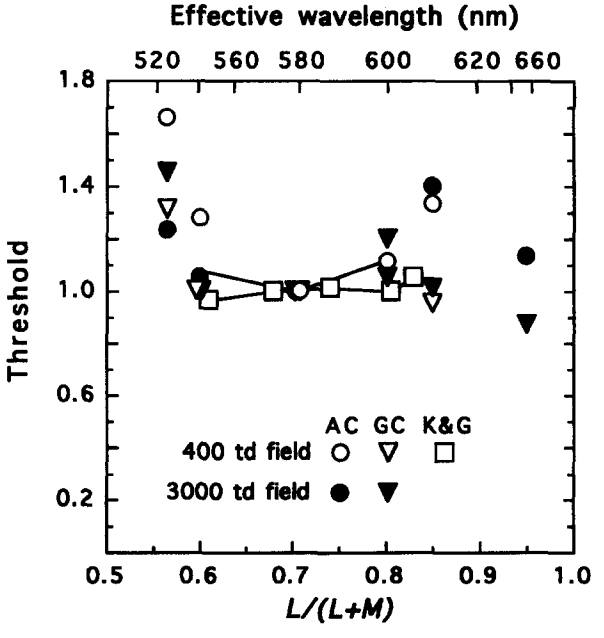

FIGURE 12. Equiluminant red–green thresholds on 400 td fields (from present study and Krausksopf and Gegenfurtner—K&G) and on 3000 td fields (present study). Bottom axis represents the horizontal axis of the MacLeod–Boynton chromaticity diagram. Thresholds are normalized to 1.0 on a yellow field. On the 400 td fields (open symbols), the equiluminant thresholds change little with field color over the field range where the two studies overlap.

two half fields matched, or the fields automatically deviated slowly from a uniform condition until the observer was satisfied that the two half fields did not match. Such experiments differ in three respects from ours and Krauskopf and Gegenfurtner's. These latter experiments employ a large uniform adapting field to which the observer is very well adapted; the equiluminant test stimulus, defined strictly in physical troland units, is presented in the center of the field, with well-controlled temporal parameters; and performance is pushed to the limit with forced-choice procedures. In the other experiments, adaptation may be less well controlled (owing to the effect of eye movements with the small field or brief field exposures), and the thresholds are often measured more subjectively.

Our less subjective methods show little variation of the equiluminant thresholds with field color, but from this alone we may not conclude that cone-selective adaptation has negligible effect on the red–green mechanism. When we transform our red–green detection contours to the cone contrast coordinates, we clearly see the roles of both cone-selective adaptation and second-site polarization (Stromeyer *et al.*, 1985). The latter occurs at an opponent site (and not within independent L and M cone pathways), since the red and green contours are displaced symmetrically from the origin while maintaining a slope of ~1.0. On the red field, for example, green flashes are no more detectable than red—whether they are signaled either by L cones or by M cones. After correcting the red and green detection contours for the second-site effect, the L cone signals and the M cone signals each reveal equivalent, Weberian adaptation over the full illuminance range.

Additional evidence for the two adaptational processes

Results with a different procedure also provide evidence for the two adaptational processes. Thornton and Pugh (1983) measured thresholds for diffuse, monochromatic incremental flashes on a large bright adapting field of 560, 580 or 600 nm. Sperling and Harwerth (1971) and King-Smith and Carden (1976) have made similar measurements. Figure 13a shows the original Thornton and Pugh thresholds measured on a 560 nm (yellow–green) and a 600 nm (orange) adapting field. In Fig. 13b these same data are transformed to cone contrast coordinates (points detected by S cones are excluded). The points lying furthest from the origin (near the 45° axis, Fig. 13b) represent test wavelengths which match the field wavelength—such a flash is a pure luminance increment. These test flashes are detected by the luminance mechanism (Calkins *et al.*, 1992), and they correspond to the points in Fig. 13a that lie deepest within the (Sloan) notches. Transforming the data to the cone contrast coordinates has distinct advantages over the format in Fig. 13a, namely: (1) the red–green contour becomes readily apparent, and we see that L and M cone contrast contribute equally to the red–green mechanism for each field condition, since a straight line fitted to the

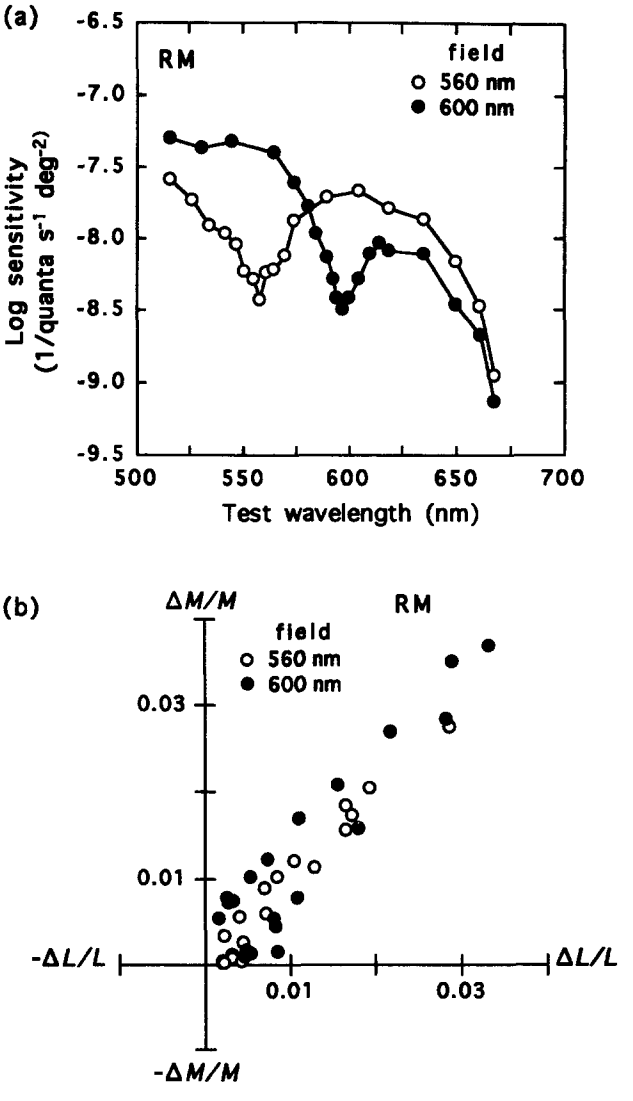

FIGURE 13. Replotted thresholds from Thornton & Pugh (1983) for diffuse, monochromatic, incremental flashes on a 560 nm (7874 td) and a 600 nm (4610 td) adapting field. (b) Same thresholds converted to cone contrast coordinates.

data would have a slope of 1.0; (2) the relative sensitivity of the luminance mechanism and red–green mechanism is made transparent (threshold vector length on +45° vs extrapolated −45° axis); and (3) the role of the second-site effect is now clear, as shown by the outward lateral shift of the contour on the 600 nm field (in Fig. 13a it is completely obscure). For observer RM, the second-site effect grew by a factor of 1.11 and 2.4, respectively, as the adapting field was changed from 560 to 580 nm and then 600 nm, showing a somewhat larger effect than our data in Fig. 5 (lower panel).

Our results and those of Thornton and Pugh show that the red–green detection contour on each colored field has a slope of ~1.0 in the cone contrast coordinates. This indicates that the L and M cones contribute with equal contrast weights in the red–green detection mechanism. Approximately equal L and M contrast weights have been observed in physiological recordings of macaque red–green retinal ganglion cells (Derrington,

Krauskopf & Lennie, 1984) and LGN cells (Lee, Martin & Valberg, 1989) using a spatially uniform test stimulus that strongly affects both the center and surround of the receptive field. Measurements were made on white or yellow fields, and it would be interesting to see if the contrast weights still remain equal on strongly colored adapting fields. Recent results by Yeh, Lee and Kremers (1995), discussed later, suggest that the weights do remain equal.

The possible sites of adaptation

Cone-selective adaptation must occur prior to the generation of a spectrally-opponent signal. In cold-blooded animals, such as turtle, there is evidence that the cone response itself may be spectrally-opponent, owing to horizontal feedback onto the cones. Burkhardt (1993) argues that this feedback plays little role in promoting color opponency, and the predominant mechanism for opponency resides beyond the cones. However, J. E. Dowling (personal communication) has pointed out that opponency at the cone level may be hard to assess, because feedback could play a significant role in controlling cone synaptic events without being seen in intracellular recordings from the cone cell body. As yet there is little direct evidence for feedback onto cones in mammals. Gross potential recordings in primates (van Norren & Baron, 1977; Sperling & Mills, 1991) suggest there may be some degree of spectral opponency as early as the bipolar cells. Cone-selective adaptation would presumably occur at the cone outer segment if there is significant horizontal feedback onto cones. If there is little such feedback and opponency is clearly present at the bipolar level, then cone-selective adaptation could be explained by adaptation at the cone–midget bipolar synapse.

We will first consider whether part of the cone-selective desensitization may be accounted for by early noise, either photon-induced or neural. We will then consider whether the cones adapt, reviewing physiological and psychophysical evidence for such a process. Finally, we will consider how the second-site effect may arise.

Noise. Increasing the intensity of a colored field might differentially increase noise within the separate L and M cone pathways, thus partly accounting for the cone-selective threshold elevation. The noise seen in the photocurrent recordings from cones (Schnapf *et al.*, 1990) increases by only a small (e.g. 80%) amount as the mean illumination is raised from dark to 400 td. However, a similar change of illumination raises the psychophysical L and M cone threshold by 60-fold (Stiles, 1961). Thus photoreceptor noise ought to have little effect on L and M cone thresholds. Neural noise may likewise be expected to have only a minor effect. The noise measured in primate retinal ganglion cells is largely constant, independent of receptive field size or type, M or P, (Croner, Purpura & Kaplan, 1993) and independent of mean adapting level (Reich, Sanchez-Vives, Mukherjee & Kaplan, 1994), leading the authors to conclude that the major source of the noise is not photon-induced but is intrinsic to the cell. Barlow and Levick (1969) originally showed that the major limitation on the reliable detection of contrast in cat retinal ganglion cells over a *large* illuminance range is not the noise (which remains almost constant, cf. Derrington & Lennie, 1982), but rather an active gain process which attenuates the incremental response approximately in proportion to the background illumination. Graham and Hood (1992) have also questioned whether photon-induced noise has a measurable visual effect at photopic levels. These studies thus suggest that noise alone likely does not account for the very *large* effects of cone-selective desensitization, even if we were to consider correlations in the noise of an ensemble of cells. We next consider whether the cones change their gain with adapting level.

Cone adaptation. The turtle cone has been studied most extensively. With increasing mean illumination, these cones strongly adapt (Normann & Perlman, 1979) and their response speeds up (Baylor & Hodgkin, 1974). The changes in the temporal impulse response (Daly & Normann, 1985) and temporal MTF (Sneyd & Tranchina, 1989) are quite similar to the concomitant changes in the human psychophysical MTF for uniform-field flicker (Kelly, 1961), thus suggesting that cone adaptation may predominantly account for changes in the temporal dynamics of human vision with adapting level (Daly & Normann, 1985). (See Shapley *et al.*, 1993, for discussion.) However, we should remark that the psychophysical inferred temporal impulse response function may also reflect receptive field properties of neurons, since the function varies strongly with spatial frequency (Watson & Nachmias, 1977).

Studies of massed potentials suggest that primate cones adapt. Baron and also Boynton (1975) and Valeton and van Norren (1983) observed that the monkey, foveal local ERG (which reflects cone activity) was strongly attenuated by increasing the steady mean illumination. The Weber-like change in sensitivity observed by Valeton and van Norren is likely caused by a time-dependent multiplicative gain change (which shifts the cone response function laterally along the illuminance axis) and, to a lesser degree, by response compression (resulting from a shift of the operating point up along the response function owing to increased hyperpolarization of the cone response). The gain change is presumably time-dependent (as manifested by the response to a non-brief test probe), for there is little evidence for static change of gain until high adapting levels are reached, as revealed by the 8-msec leading edge of the cone *a*-wave (Hood & Birch, 1993). It has been pointed out (Shapley *et al.*, 1993; Hood & Birch, 1993) that the change in cone sensitivity observed by Valeton and van Norren is somewhat less than is needed to explain the psychophysical increment threshold. However, Seiple, Holopigian, Greenstein and Hood (1992) recently showed a close concurrence between human flicker sensitivity (>20 Hz) measured psychophysically and the focal ERG. They concluded that most of the adaptation-dependent change in sensitivity occurs at the cones or cone–bipolar synapse. The lack of cone

adaptation seen by Schnapf *et al.* (1990) in the photocurrent recordings of excised primate cones might reflect an altered extracellular milieu (Seiple *et al.*, 1992). Quite likely, these measurements would not reveal adaptation manifested by a voltage-controlled conductance change at the inner segment which may affect presynaptic potentials or modify the release of neurotransmitter at the cone–bipolar synapse (cf. Walraven, Enroth-Cugell, Hood, MacLeod & Schnapf, 1990).

Recent psychophysical studies on cone adaptation "pools" show that the spatial spread of light adaptation is confined to a single cone. Cicerone, Hayhoe and MacLeod (1990) demonstrated that the spread of bleaching adaptation with a grating was only 1 cone wide at a parafoveal locus, whereas the neural summation was 5 cones wide, thus placing the site of adaptation at the cone itself. MacLeod, Williams and Makous (1992) concluded that, in the fovea, adaptation was very local (1 cone wide) based on the visibility of nonlinear spatial beats formed between an interference grating (which was well above the spatial resolution limit) and the *after-image* of a similar high-frequency grating. This early site of light adaptation obeys Weber's Law at mean levels above ~ 100 td, since the deduced nonlinear response function (which gives rise to the beats) has the same shape when measured with gratings of *constant contrast* at each adapting level (Makous, Williams & MacLeod, 1995). These studies thus also support the view that considerable light adaptation occurs either within single cones or at the junction between a single cone and its midget bipolar cell (MacLeod *et al.*, 1992). Adaptation at such a site could explain our observation of cone-selective chromatic adaptation.

Second-site adaptation. If the L and M cones completely adapt, can there remain a color signal to polarize the second-site? Imagine that adaptation acted like a neutral filter placed selectively over the L and the M cones so as to mimic the attenuation of the cone signals by the colored adapting field. Then a red field might be expected to turn yellow (since the L cones would be more filtered than the M cones), and a red signal would not be available to polarize the second-site. Such a "dark glass" model of adaptation is inconsistent with physiology, for adapting fields do not produce simply a "static" gain change (Hood & Birch, 1993).

The cones may adapt to each increasing mean level, producing Weber-like behavior for small incremental flashes. This may arise from a combination of gain change and weak response compression, but information about the mean level is *not* lost, since the photoreceptor becomes increasingly hyperpolarized as the steady illumination is raised (Kleinschmidt & Dowling, 1975; Normann & Perlman, 1979; Valeton & van Norren, 1983). This preservation of information about mean level further shows the "dark glass" model must be wrong. The red field will thus hyperpolarize the L cones more than the M cones, and this difference may result in a "red" signal for the second-site. The steady field must be of long wavelength (> 580 nm) to produce the second-site desensitization, for a yellow (575 nm) retinally-stabilized field can be made to appear uniformly red by filling-in from an unstabilized red surround, yet this has *no* effect on the chromatic threshold; conversely a long-wavelength red field can be made to appear yellow by filling-in from a yellow surround, and this likewise has no effect on threshold (Nerger, Piantanida & Larimer, 1993).

It might be argued that the *steady* (hyperpolarized) cone signals would not penetrate deeper into the visual system to polarize the second-site. However, several psychophysical studies indicate that steady cone signals can propagate to the bipolar cells or beyond. Hayhoe (1979) showed that a small-field bleach or stabilized image (Hayhoe & Smith, 1989) strongly elevated the threshold of a tiny test flash centered on the field, even after the stabilized field faded. The persisting cone signal may produce desensitization by over-driving the bipolar cells, since the ganglion cells would be poorly stimulated by steady (retinally-stabilized) fields (Hayhoe, 1979). Our second-site effect could also arise at the bipolar level, since bipolar cells appear to be spectrally-opponent to some degree (van Norren & Baron, 1977; Sperling & Mills, 1991).

Other studies suggest that steady cone signals may propagate further than the bipolar cells. DeValois and Walraven (1967) showed that a red bleach in one eye changed the color of the field seen with the *other* eye for 3 min following the bleach, even though the bleach after-image itself could only be seen for a brief period, since it was retinally stabilized.

Recently, Yeh *et al.* (1995) demonstrated clear effects of *steady* chromatic fields on the response of macaque red–green ganglion cells. Red and green–yellow (~ 1100 td) fields were interchanged as infrequently as every $2\frac{1}{2}$ min. Strong, sustained suppression was observed over the entire period during presentation of the field color that inhibited the cell. Suppression could be induced through either cone type, e.g. a $+M-L$ cell could be suppressed by decrementing M-cone field stimulation or by incrementing L-cone field stimulation. The change in sensitivity was highly similar whether probed with an L-cone or M-cone test stimulus; the cone contrast gain was similar for both L test stimuli and M test stimuli. As the authors state, independent adjustment of L and M cone contrast gain likely occurs before an opponent site, whereas the persistent chromatic suppression reflects activity at an opponent site.

In conclusion, the colored adapting field may differently hyperpolarize the L and M cones, and persisting signal from these cones may polarize the second site. This difference in cone hyperpolarization is consistent with the equivalent Weberian adaptation of the L and M cones.

Unique yellow settings and Weberian adaptation in the red–green detection mechanism

We conclude that the red–green detection mechanism shows close adherence to Weber's Law, for L and M cone contrast contributed equally to red–green detection

on each colored field (providing the adapting field was sufficiently intense). Thus the red–green detection contour (in cone contrast coordinates) has a slope of ~1.0—parallel to the +45°, luminance axis. A suprathreshold flash on the luminance axis appears about the same color as the adapting field—the flash matches the field wavelength and produces only a luminance change.

Ahn and MacLeod (1993) have used a very different technique to assess the degree of Weberian adaptation of the L and M inputs to the red–green mechanism. They set incremental flashes (a mixture of red and green light) to appear unique yellow on different colored fields. Figure 14 shows some of these results transformed to cone contrast coordinates, so as to illustrate the observed shortfall from Weberian adaptation. As the adaptation field is made more intense, the vectors more closely approach the 45° luminance axis. The vectors for the most intense fields represent the *asymptotic* approach seen in the similar results of Walraven (1981). The vectors never reach the 45° axis. Walraven predicts that if there is Weberian cone adaptation (and the background is fully discounted), then unique yellow will lie on the 45° axis (see his Fig. 7).

Our results on the red–green detection mechanism suggest that the cones do independently adapt, obeying Weber's Law, for the contour slope is 1.0, parallel to the luminance axis. According to our view, a suprathreshold flash which has no red–green valence *relative to the adapting field* represents a pure luminance flash matching the field chromaticity—not a unique yellow flash.

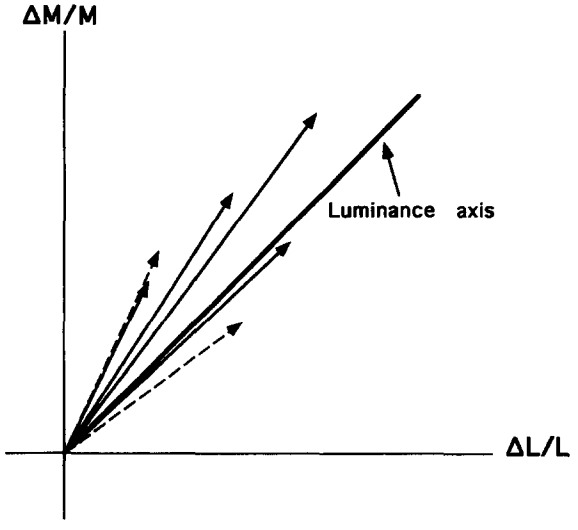

FIGURE 14. Weberian shortfall for unique yellow settings. Vectors above the 45° luminance axis represent unique yellow settings on red fields; vectors below the axis represent settings on green fields. Relative vector length indicates increased adapting illuminance. Even for the brightest fields, the vectors fall short of the 45° axis. All test stimuli were flashed at ~50 × threshold. [Low intensity flashes may produce greater tilt away from the 45° axis, according to Shevell (1978)]. Solid vectors from Walraven (1981): adapting field red (640 nm; 100, 3000 and 10,000 td) or green (555 nm; 3000 td). Dashed vectors from Ahn and MacLeod (1993—observer SA): adapting field red (640 nm; 800 td) or green (530 nm; 800 td).

Unique yellow flashes, which are considerably suprathreshold (Shevell, 1978), may lie along an approximately straight line that is *tilted off* this luminance axis. The vectors in Fig. 14 are tilted sufficiently so that they will cross the red–green detection contour and thus produce a response in this mechanism even though the flashes appear unique yellow on the *red* or *green* adapting fields. Thus on red or green adapting fields unique yellow increments do not necessarily reflect a null for the red–green detection mechanism.

REFERENCES

Ahn, S. J. & MacLeod, D. I. A. (1993). Link-specific adaptation in the luminance and chromatic channels. *Vision Research, 33*, 2271–2286.

Barlow, H. B. & Levick, W. R. (1969). Three factors limiting the reliable detection of light by retinal ganglion cells of the cat. *Journal of Physiology, London, 200*, 1–24.

Baron, W. S. & Boynton, R. M. (1975). Response of primate cones to sinusoidally flickering homochromatic stimuli. *Journal of Physiology, London, 246*, 311–331.

Baylor, D. A. & Hodgkin, A. L. (1974). Changes in time scale and sensitivity in turtle photoreceptors. *Journal of Physiology, London, 242*, 729–758.

Bedford, R. E. & Wyszecki, G. (1957). Axial chromatic aberration of the human eye. *Journal of the Optical Society of America, 47*, 564–567.

Boynton, R. M. (1986). A system of photometry and colorimetry based on cone excitations. *Color Research and Application, 11*, 244–252.

Boynton, R. M. & Kambe, N. (1980). Chromatic difference steps of moderate size measured along theoretically critical axes. *Color Research and Application, 5*, 13–23.

Brown, W. R. J. & MacAdam, D. L. (1949). Visual sensitivities to combined chromaticity and luminance differences. *Journal of the Optical Society of America, 39*, 808–834.

Burkhardt, D. A. (1993). Synaptic feedback, depolarization, and color opponency in cone photoreceptors. *Visual Neuroscience, 10*, 981–989.

Calkins, D. J., Thornton, J. E. & Pugh, E. N. Jr (1992). Monochromatism determined at a long-wavelength/middle-wavelength cone-antagonistic locus. *Vision Research, 32*, 2349–2367.

Chaparro, A., Stromeyer, C. F. III, Huang, E. P., Kronauer, R. E. & Eskew, R. T. Jr (1993). Colour is what the eye sees best. *Nature, 361*, 348–350.

Chaparro, A., Stromeyer, C. F. III, Kronauer, R. E. & Eskew, R. T. Jr (1994). Separable red–green and luminance detectors for small flashes. *Vision Research, 34*, 751–762.

Cicerone, C. M., Hayhoe, M. M. & MacLeod, D. I. A. (1990). The spread of adaptation in human foveal and parafoveal cone vision. *Vision Research, 30*, 1603–1615.

Cole, G. R., Stromeyer, C. F. III & Kronauer, R. E. (1990). Visual interactions with luminance and chromatic stimuli. *Journal of the Optical Society of America A, 7*, 128–140.

Cole, G. R., Hine, T. & McIlhagga, W. (1993). Detection mechanisms in L-, M-, and S-cone contrast space. *Journal of the Optical Society of America A, 10*, 38–51.

Croner, L. J., Purpura, K. & Kaplan, E. (1993) . Response variability in retinal ganglion cells of primates. *Proceedings of the National Academy of Science, 90*, 8128–8130.

Daly, S. & Normann, R. A. (1985). Temporal information processing in cones: effects of light adaptation on temporal summation and modulation. *Vision Research, 25*, 1197–1206.

Derrington, A. M. & Lennie, P. (1982). The influence of temporal frequency and adaptation level on receptive field organization of retinal ganglion cells in cat. *Journal of Physiology, London, 333*, 343–366.

Derrington, A. M., Krauskopf, J. & Lennie, P. (1984). Chromatic mechanisms in lateral geniculate nucleus of macaque. *Journal of Physiology, London, 357*, 241–265.

DeValois, R. L. & Walraven, J. (1967). Monocular and binocular aftereffects of chromatic adaptation. *Science, New York, 155*, 463–465.

Eisner, A. & MacLeod, D. I. A. (1981). Flicker photometric study of chromatic adaptation: selective suppression of cone inputs by colored backgrounds. *Journal of the Optical Society of America, 71*, 705–718.

Eskew, R. T. Jr, Stromeyer, C. F. III & Kronauer, R. E. (1992). The constancy of equiluminant red–green thresholds examined in two color spaces. *Advances in Color Vision (Optical Society of America), 4*, 195–197.

Graham, N. & Hood, D. C. (1992). Quantal noise and decision rules in dynamic models of light adaptation. *Vision Research, 33*, 779–787.

Hayhoe, M. M. (1979). After-effects of small adapting fields. *Journal of Physiology, London, 296*, 141–158.

Hayhoe, M. M. & Smith, M. V. (1989). The role of spatial filtering in sensitivity regulation. *Vision Research, 29*, 457–469.

Hood, D. C. & Birch, D. G. (1993). Human cone receptor activity: the leading edge of the *a*-wave and models of receptor activity. *Visual Neuroscience, 10*, 857–871.

Ives, H. E. (1912). The relation between the color of the illuminant and the color of the illuminated object. *Transactions of the Illuminating Engineers Society, 7*, 62–72.

Kelly, D. H. (1961). Visual responses to time-dependent stimuli. I. Amplitude sensitivity measurements. *Journal of the Optical Society of America, 51*, 422–429.

King-Smith, P. E. & Carden, D. (1976). Luminance and opponent-color contributions to visual detection and adaptation and to temporal and spatial integration. *Journal of the Optical Society of America, 66*, 709–717.

Kleinschmidt, J. & Dowling, J. E. (1975). Intracellular recordings from gecko photoreceptors during light and dark adaptation. *Journal of General Physiology, 66*, 617–648.

Krauskopf, J. & Gegenfurtner, K. (1992). Color discrimination and adaptation. *Vision Research, 32*, 2165–2175.

Lamb, T. D. (1985). Properties of cone photoreceptors in relation to colour vision. In Ottoson, D. & Zeki, S. (Eds), *Central and peripheral mechanisms of color vision*. London: Macmillan.

Lee, B. B., Martin, P. R. & Valberg, A. (1989). Sensitivity of macaque retinal ganglion cells to chromatic and luminance flicker. *Journal of Physiology, London, 414*, 223–243.

LeGrand, Y. (1949). Les seuils différentiels de couleurs dans la théorie de Young. *Revue d'Optique Théoretique et Instrumentate, 28*, 261–278.

MacAdam, D. L. (1942). Visual sensitivities to color differences in daylight. *Journal of the Optical Society of America, 32*, 247–273.

MacLeod, D. I. A. & Boynton, R. M. (1979). Chromaticity diagram showing cone excitation by stimuli of equal luminance. *Journal of the Optical Society of America, 69*, 1183–1186.

MacLeod, D. I. A., Williams D. R. & Makous, W. (1992). A visual nonlinearity fed by single cones. *Vision Research, 32*, 347–363.

Makous, W., Williams, D. R. & MacLeod, D. I. A. (1995). Early visual nonlinearity and adaptation. In preparation.

Nagy, A. L., Eskew, R. T. Jr & Boynton, R. M. (1987). Analysis of color-matching ellipses in a cone-excitation space. *Journal of the Optical Society of America A, 4*, 756–768.

Nerger, J. L., Piantanida, T. P. & Larimer, J. (1993). Color appearance of filled-in backgrounds affects hue cancellation, but not detection thresholds. *Vision Research, 33*, 165–172.

Normann, R. A. & Perlman, I. (1979). The effects of background illumination on the photoresponses of red and green cones. *Journal of Physiology, London, 286*, 491–507.

Normann, R. A., Perlman, I. & Hallett, P. E. (1991). Cone photoreceptor physiology and cone contributions to colour vision. In Gouras P. (Ed.) *Vision and visual dysfunction*, Vol. 6, *The perception of colour* (pp. 146–162). New York: Macmillan.

van Norren, D. & Baron, W. S. (1977). Increment spectral sensitivities of the primate late receptor potential and *b*-wave. *Vision Research, 17*, 807–810.

Pugh, E. N. Jr & Mollon, J. D. (1979). A theory of the π_1 and π_3 color mechanisms of Stiles. *Vision Research, 19*, 293–312.

Purpura, K., Tranchina, D., Kaplan, E. & Shapley, R. M. (1990). Light adaptation in the primate retina: analysis of changes in gain and dynamics of monkey retinal ganglion cells. *Visual Neuroscience, 4*, 75–93.

Reich, D. S., Sanchez-Vives, M. Mukherjee, P. & Kaplan, E. (1994). Response variability of retinal ganglion cells is independent of the synaptic pathway activated and of retinal illumination. *Investigative Ophthalmology & Visual Science, 35 (Suppl.)*, 2124.

Romero, J., García, J. A., Jiménez del Barco, L. & Hita, E. (1993). Evaluation of color-discrimination ellipsoids in two-color spaces. *Journal of the Optical Society of America A, 10*, 827–837.

Schnapf, J. L., Nunn, B. J., Meister, M. & Baylor, D. A. (1990). Visual transduction in the cones of the monkey *Macaca fascicularis*. *Journal of Physiology, London, 427*, 681–713.

Seiple, W., Holopigian, K., Greenstein, V. & Hood, D. C. (1992). Temporal frequency dependent adaptation at the level of the outer retina in humans. *Vision Research, 32*, 2043–2043.

Shapley, R. & Enroth-Cugell, C. (1984). Visual adaptation and retinal gain controls. In Osborne, N. N. & Chader, G. J. (Eds), *Progress in retinal research* (Vol. 3, pp. 263–346). Oxford: Pergamon.

Shapley, R. & Kaplan, E. (1990). Tonic suppressive interactions between center and surround in P ganglion cells and parvocellular neurons. *Investigative Ophthalmology & Visual Science, 31 (Suppl.)*, 88.

Shapley, R., Kaplan, E. & Purpura, K. (1993). Contrast sensitivity and light adaptation in photoreceptors or in the retinal network. In Shapley, R. & Lam, D. M.-K. (Eds), *Contrast sensitivity* (pp. 103–116). Cambridge: M.I.T. Press.

Shevell, S. K. (1978). The dual role of chromatic backgrounds in color perception. *Vision Research, 18*, 1649–1661.

Smith, V. C. & Pokorny, J. (1975). Spectral sensitivity of the foveal cone photopigments between 400 and 500 nm. *Vision Research, 15*, 161–171.

Sneyd, J. & Tranchina, D. (1989). Phototransduction in cones: an inverse problem in enzyme kinetics. *Bulletin of Mathematical Biology, 51*, 749–784.

Sperling, H. G. & Harwerth, R. S. (1971). Red–green cone interactions in the increment-threshold spectral sensitivity of primates. *Science, New York, 172*, 180–184.

Sperling, H. G. & Mills, S. L. (1991). Red–green interactions in the spectral sensitivity of primates as derived from ERG and behavioral data. *Visual Neuroscience, 7*, 75–86.

Stiles, W. S. (1961). Adaptation, chromatic adaptation, colour transformation. *Anales Real de la Sociada Española de Fisica y Quimica, A57*, 149–175.

Stiles, W. S. (1978). *Mechanisms of colour vision*. New York: Academic Press.

Stromeyer, C. F. III, Cole, G. R. & Kronauer, R. E. (1985). Second-site adaptation in the red–green chromatic pathways. *Vision Research, 25*, 219–237.

Stromeyer, C. F. III, Cole, G. R. & Kronauer, R. E. (1987). Chromatic suppression of cone inputs to the luminance flicker mechanism. *Vision Research 27*, 1113–1137.

Swanson, W. H., Pokorny, J. & Smith, V. C. (1988). Effects of chromatic adaptation on phase-dependent sensitivity to heterochromatic flicker. *Journal of the Optical Society of America A, 5*, 1976–1982.

Thornton, J. E. & Pugh, E. N. Jr (1983). Red/green color opponency at detection threshold. *Science, New York, 219*, 191–193.

Valeton, J. M. & van Norren, D. (1983). Light adaptation of primate cones: an analysis based on extracellular data. *Vision Research, 23*, 1539–1547.

Walraven, J. (1981). Perceived colour under conditions of chromatic adaptation: evidence for gain control by π mechamisms. *Vision Research, 21*, 611–620.

Walraven, J., Enroth-Cugell, C., Hood, D. C., MacLeod, D. I. A. & Schnapf, J. L. (1990). The control of visual sensitivity: receptoral

and postreceptoral processes. In Spillmann, L. & Werner, J. S. (Eds), *Visual perception: The neurophysiological foundations* (pp. 53–101). San Diego: Academic Press.

Wandell, B. A. & Pugh, E. N. Jr (1980). Detection of long-duration, long-wavelength incremental flashes by a chromatically coded pathway. *Vision Research, 20*, 625–636.

Watson, A. B. & Nachmias, J. (1977). Patterns of temporal interaction in the detection of gratings. *Vision Research, 17*, 893–902.

Watson, A. B. & Pelli, D. G. (1983). QUEST: a Bayesian adaptive psychometric method. *Perception & Psychophysics, 33*, 113–120.

Wyszecki, G. & Fielder, G. H. (1971). New color matching ellipses. *Journal of the Optical Society of America, 61*, 1135–1152.

Yeh, T., Lee, B. B. & Kremers, J. (1995). The time course of adaptation in macaque retinal ganglion cells. In preparation.

Acknowledgements—Research supported by NIH EY 01808, AFOSR 89-0304 and Ford Foundation. We thank D. Hood, B. B. Lee, W. Makous, R. Shapley and S. Shevell for comments.